

# A BIREFRINGENCE RELAXATION DETERMINATION OF ROTATIONAL DIFFUSION OF MAGNETOTACTIC BACTERIA

CHARLES ROSENBLATT,\* RICHARD B. FRANKEL,\* AND RICHARD P. BLAKEMORE†

\*Francis Bitter National Magnet Laboratory, Massachusetts Institute of Technology, Cambridge, Massachusetts 02139; and †Department of Microbiology, University of New Hampshire, Durham, New Hampshire 03824

**ABSTRACT** The orientational relaxation of the magnetotactic bacterium *Aquaspirillum magnetotacticum* is observed by the decay of the optical birefringence upon switching off an aligning magnetic field. The data yield a rotational diffusion constant  $D_r \approx 0.13 \text{ s}^{-1}$  and information about cell sizes that is consistent with optical microscopy data.

The magnetotactic bacterium *Aquaspirillum magnetotacticum* (*A. magnetotacticum*) contains a chain of single magnetic-domain magnetite particles that imparts a magnetic dipole moment  $\mu$  to the cell parallel to the axis of motility; the cell thus orients and swims along the earth's magnetic-field lines (1–3). The directionally averaged velocity  $\langle V \rangle$  is determined from the classical Boltzmann orientational distribution, and is given by  $\langle V \rangle = V_0 \cdot \langle \cos \theta \rangle$ , where

$$\langle \cos \theta \rangle = [\coth(\mu H/k_B T) - k_B T/\mu H]. \quad (1)$$

Here  $k_B$  is Boltzmann's constant,  $T$  is temperature, and  $\theta$  is the angle between the instantaneous trajectory and  $\mathbf{H}$ . If the swimming direction is somehow disturbed, a bacterium will feel a magnetic torque and right itself. Opposing the reorientation will be a viscous drag such that

$$\frac{k_B T}{D_r} \frac{d\theta}{dt} + \mu H \sin \theta = 0, \quad (2)$$

where  $D_r$  is the rotational diffusion constant. If the initial perturbed angle  $\theta_i$  is small, the reorientation will take place on a characteristic time scale

$$\tau = \frac{k_B T}{\mu H D_r}. \quad (3)$$

Note that Brownian motion, which is responsible for  $\langle \cos \theta \rangle \neq 1$  in Eq. 1, contributes an additional term to Eq. 2.

In this article we report on measurements of rotational diffusion using the method of birefringence relaxation. Because of its permanent magnetic dipole moment, *A. magnetotacticum* can be oriented within a very small solid angle about a given direction defined by an external magnetic field  $\mathbf{H}_{\text{ex}}$ . Moreover, oriented bacteria give rise to an optical birefringence  $\Delta n$  (4). When  $\mathbf{H}_{\text{ex}}$  is set equal to

zero, the orientations of the cells randomize, resulting in a decay of the optical birefringence  $\Delta n$ . Since  $\Delta n \propto \langle P_2(\cos \theta) \rangle = \langle 3/2 \cos^2 \theta - 1/2 \rangle$ , where  $\langle \rangle$  represents an ensemble average, measurements of  $\Delta n$  vs. time yield information about orientational diffusion.

Although the bacteria are actually helical in shape with a relatively small length to pitch ratio, certain approximations are used to fit the data. The simplest approximation is to assume that the bacteria are cylindrical with all principal axes of the optical anisotropy and rotational diffusion tensors coinciding. In this case both tensors are uniaxial (5) and the birefringence relaxation is determined by a single-exponential term (5, 6)

$$\Delta n = \Delta n_0 \exp(-6D_r t), \quad (4)$$

where  $\Delta n_0$  is a function of  $H_{\text{ex}}$  before the external field is turned off and  $D_r$  is the rotational diffusion constant about an axis perpendicular to the cylindrical axis. The diffusion constant  $D_r$  can be written as (7)

$$D_r = \frac{3k_B T}{\pi \eta L^3} \left( \ln \frac{L}{d} - \gamma \right), \quad (5)$$

where  $\eta$  is the viscosity of the medium,  $L$  the length of the cylinder, and  $d$  the width. End effects are treated by the parameter  $\gamma$ , which depends upon the aspect ratio  $L/d$  and for which there is, unfortunately, no theoretical consensus (7). For sufficiently large  $L/d$ , the  $\gamma$  term becomes inconsequential; nevertheless, for *A. magnetotacticum* the ratio  $L/d$  is of order 5 to 10, and thus  $\gamma$  is not insignificant. For purposes of data analysis, we have chosen to use the form of Tirado and de la Torre (8)

$$\gamma = 0.662 - 0.92 (d/L). \quad (6)$$

This form produces reasonable results for small aspect

ratios. Other forms for  $\gamma$  (7) produce only slightly different final results.

Cells of *A. magnetotacticum* were grown in culture and then killed and fixed with a small amount of glutaraldehyde. Cell concentration was  $\sim 2 \times 10^8 \text{ ml}^{-1}$ . By measuring the static birefringence (4) vs.  $H_{ex}$ ,  $\langle \mu \rangle$  was found to be  $2.6 \times 10^{-13} \text{ emu}$  with a distribution width of  $\pm 1.7 \times 10^{-13} \text{ emu}$ . Thus, even in a field as small as 1 G we find from Eq. 1 that  $\langle \cos \theta \rangle > 0.8$ . The sample was then placed in a glass cuvette of pathlength 1 cm, which in turn was placed between a pair of Helmholtz coils housed in a mu-metal can. The ambient field inside the can was  $< 0.01 \text{ G}$ . The entire assembly was then inserted into an optical birefringence apparatus, described in detail elsewhere (4). The field was brought to a steady-state value  $H_{ex}$  and then switched off; the transient birefringence was recorded with a Biomation model 1015 waveform recorder (Biomation Inc., Palo Alto, CA) and then output into an xy plotter.

A typical trace is shown in Fig. 1, where the initial field  $H_{ex}$  was 8 G. To within the expected scale factor, data taken at fields  $0.24 \text{ G} \leq H_{ex} \leq 40 \text{ G}$  produced virtually identical traces, as expected from Eq. 4. In Fig. 2 we have digitized the data and plotted the results on a semilog scale. Owing to the nonlinearity of this curve, it is clear that there is a distribution in  $D_r$  arising from a polydispersity of cell lengths  $L$ . Although there is no a priori form expected for the length distribution, a Gaussian was chosen for convenience

$$f(L) = \frac{1}{\Delta L \sqrt{\pi}} e^{-(L-L_0)^2/\Delta L^2}. \quad (7)$$

$L_0$  is the average length and  $\Delta L$  the width of the distribution. Thus, combining Eqs. 4 and 7, we find the transient birefringence behaves as

$$\Delta n \propto \int dL \left( \frac{L}{d} - 1 \right) e^{-6D_r t} f(L), \quad (8)$$

where  $D_r$  is given by Eqs. 5 and 6 and  $d$  is fixed at the

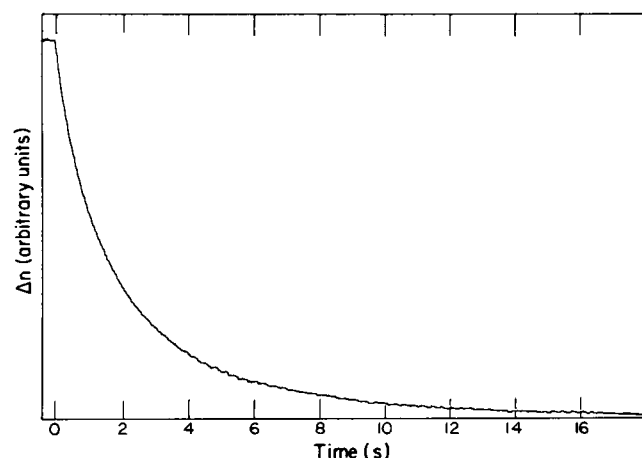


FIGURE 1 The typical decay of birefringence for initial aligning field  $H_{ex} = 8 \text{ G}$  is shown.

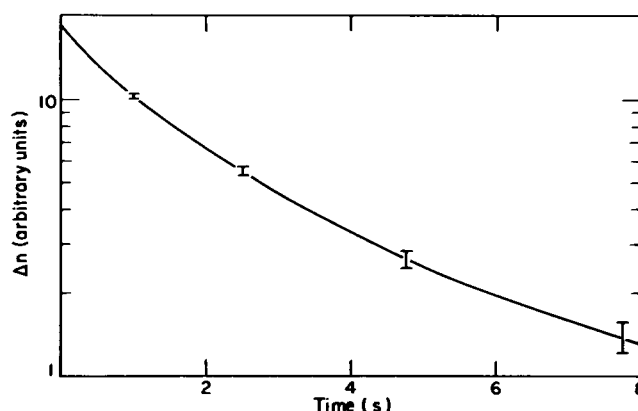


FIGURE 2 Fig. 1 is redrawn on a semilog plot. Note the nonlinearity, which indicates a distribution of effective diffusion constants. Error bars arise from uncertainty in locating base line.

experimental value of  $0.56 \mu\text{m}$  (9). The term  $(L/d) - 1$  is an approximate form that mimics the shape birefringence of a bacterium with an aspect ratio  $L/d$ .

The three parameters  $L_0$ ,  $\Delta L$ , and the coefficient in Eq. 8 were fit to several sets of data taken at various initial fields  $H_{ex}$ . All traces produced similar results with  $L_0 = 3.4 \pm 0.5 \mu\text{m}$  and  $\Delta L = 2.1 \pm 0.6 \mu\text{m}$ . Thus, for  $L = L_0$ ,  $D_r = 0.13 \text{ s}^{-1}$ . Note that the correction term  $\gamma$  in Eq. 5 is of order one-third the value of  $\ln L/d$  owing to the small aspect ratio.

The diffusion results for  $L_0$  and  $\Delta L$  were then compared

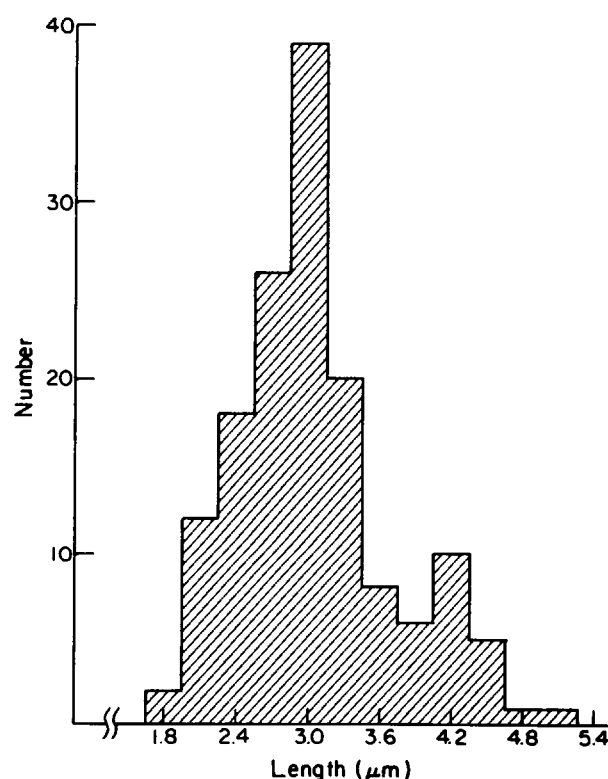


FIGURE 3 End-to-end length distribution of a sample of 148 cells is shown.

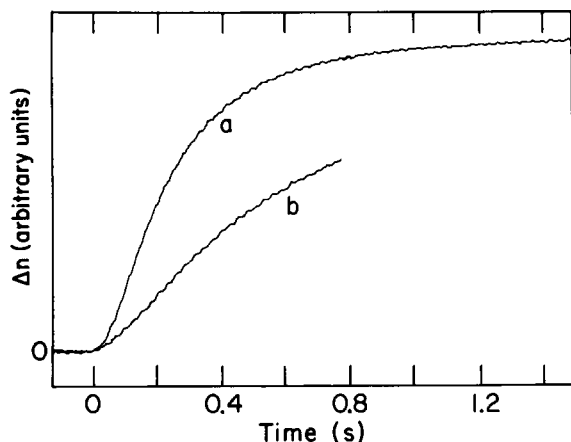


FIGURE 4  $\Delta n$  vs. time upon switching on a field  $H_0$  is shown; (a) 12.7 G; (b) 4.8 G.

with direct measurements of cell length. Photographs of 148 cells sandwiched between a pair of microscope slides spaced 1  $\mu\text{m}$  apart were taken using a phase contrast microscope and measured for their end-to-end lengths. The distribution is shown in Fig. 3. From these measurements an average length  $L_0 = (3.0 \pm 0.3) \mu\text{m}$  was determined, with a distribution width of  $\sim 2\Delta L = 1.8 \mu\text{m}$ . Although the measured length compares favorably with that obtained from the rotational diffusion measurements, the actual distribution width is somewhat narrower. To a great extent these differences have arisen from the choice of a cylindrical model for the bacteria (10). In fact, the cells are helical in shape, and thus for a sufficiently short length-to-pitch ratio the uniaxial approximation breaks down. The model also disregards coupling between rotational and translational diffusion, which at best is only a fair approximation given the shape of the bacteria. Finally, the results depend (albeit only weakly) upon the form chosen for  $\gamma$ . Unfortunately, there is no theoretical treatment of  $D_r$  for particles having the shape of these bacteria, and thus we chose to rely upon the cylindrical model.

The final question to be addressed is how  $D_r$  relates to the reorientation time  $\tau$ . In Fig. 4 we show  $\Delta n$  vs.  $t$  when  $H_{ex}$  is switched from zero to some field  $H_0$  ( $H_0 = 12.7$  [a] and  $H_0 = 4.8$  [b]) at  $t = 0$ . From Eq. 2 we find for a strong (saturating) field that

$$\theta(t) = 2 \left[ \tan^{-1} \left( e^{-t/\tau} \tan \frac{\theta_i}{2} \right) \right]. \quad (9)$$

Since  $\theta_i$  is randomly distributed for  $t < 0$ ,  $\Delta n$  vs.  $t$  can be calculated using Eq. 9

$$\Delta n(t) = 1/2 \int_0^\pi \Delta n_0 \left[ \frac{3}{2} \cos^2 \theta(t) - \frac{1}{2} \right] \sin \theta_i d\theta_i. \quad (10)$$

Owing to the dependence of  $\tau$  on  $\mu$ , Eq. 10 implicitly assumes a knowledge of the distribution in  $\mu$  as well as the distribution in  $L$ . Because of this additional uncertainty, we have not performed a full analysis of the data in Fig. 4. If,

however, we make the simplifying assumptions that both the  $\mu$  and  $L$  distributions are narrow and the system can be described by a single value for  $D_r$ , Fig. 4 can be fit to Eqs. 9 and 10. For trace a, for example, we find  $\tau = 0.11 \pm 0.04$  s. Working backwards and assuming  $\mu = 2.6 \times 10^{-13}$  emu, we find from Eq. 3 that  $D_r \approx 0.11 \text{ s}^{-1}$ , which compares favorably with the decay results.

In New England, where *A. magnetotacticum* was originally isolated, the geomagnetic field  $H_G = 0.5$  G. Since the characteristic reorientation time for  $H_G$  is  $\tau = 2.5$  s (see Eq. 3) and *A. magnetotacticum* swims at  $\sim 40 \mu\text{m/s}$ , an orientationally perturbed cell will travel a short characteristic distance  $\lambda = 90 \mu\text{m}$  before its velocity is brought into alignment with  $H_G$ . On the other hand, if a somewhat larger organism ( $L_0 \sim 20 \mu\text{m}$ ) possessing the same moment  $\mu$  and swimming speed  $V_0$  were subjected to a disturbance, the characteristic reorientation length  $\lambda$  would be nearly 3 cm, apparently compromising the utility of magnetotaxis. It is perhaps for these dynamic reasons that larger microorganisms such as the one described by Esquivel et al. (11) have been found to possess significantly larger magnetic moments.

C. Rosenblatt and R. B. Frankel were supported in part by Office of Naval Research Contract N00014-80-C-0256 and R. P. Blakemore was supported in part by National Science Foundation Grant PCM-8215900. The Francis Bitter National Magnet Laboratory is supported by the National Science Foundation through its Division of Materials Research under Contract DMR-8211416.

Received for publication 10 July 1984.

## REFERENCES

1. Blakemore, R. P. 1975. Magnetotactic bacteria. *Science (Wash. DC)*. 190:377-379.
2. Frankel, R. B., R. P. Blakemore, and R. S. Wolfe. 1979. Magnetite in freshwater magnetotactic bacteria. *Science (Wash. DC)*. 203:1355-1356.
3. Frankel, R. B. 1984. Magnetic guidance of organisms. *Annu. Rev. Biophys. Bioeng.* 13:85-103.
4. Rosenblatt, C., F. F. Torres de Araujo, and R. B. Frankel. 1982. Birefringence determination of magnetic moments of magnetotactic bacteria. *Biophys. J.* 40:83-85.
5. Wegener, W. A., R. M. Dowben, and V. J. Koester. 1979. Time-dependent birefringence, linear dichroism, and optical rotation resulting from rigid-body rotational diffusion. *J. Chem. Phys.* 70:622-623.
6. Ridgeway, D. 1966. Transient electric birefringence of suspensions of asymmetric ellipsoids. *J. Am. Chem. Soc.* 1966:1104-1112.
7. Elias, J. G., and D. Eden. 1981. Transient electric birefringence study of length and stiffness of short DNA restriction fragments. *Biopolymers*. 20:2369-2380.
8. Tirado, M. M., and J. G. de la Torre. 1980. Rotation dynamics of rigid, symmetric top macromolecules. Application to circular cylinders. *J. Chem. Phys.* 73:1986-1993.
9. Balkwill, D. L., D. Maratea, and R. P. Blakemore. 1980. Ultrastructure of magnetotactic spirillum. *J. Bacteriol.* 141:1399-1408.
10. de la Torre, J. G., and V. A. Bloomfield. 1981. Hydrodynamic properties of complex, rigid, biological macromolecules. Theory and applications. *Q. Rev. Biophys.* 14:81-139.
11. Esquivel, D. M. S., H. C. P. Lins de Barros, M. Farina, P. H. A. Aragao, and J. Danon. 1983. Microorganisms magnetotactiques de la region de Rio de Janeiro. *Biol. Cell.* 47:227-234.